APPENDICES

APPENDIX A

SUPPLEMENTARY RESULTS

A.1 PFM amplitude and phase and PR response loop of PZT (standard sample)

The results displayed in the figure confirm the functionality and accuracy of our Piezoresponse Force Microscopy (PFM) setup by measuring a standard PZT sample, which is well-known for its ferroelectric properties. Here's a detailed explanation of each panel.
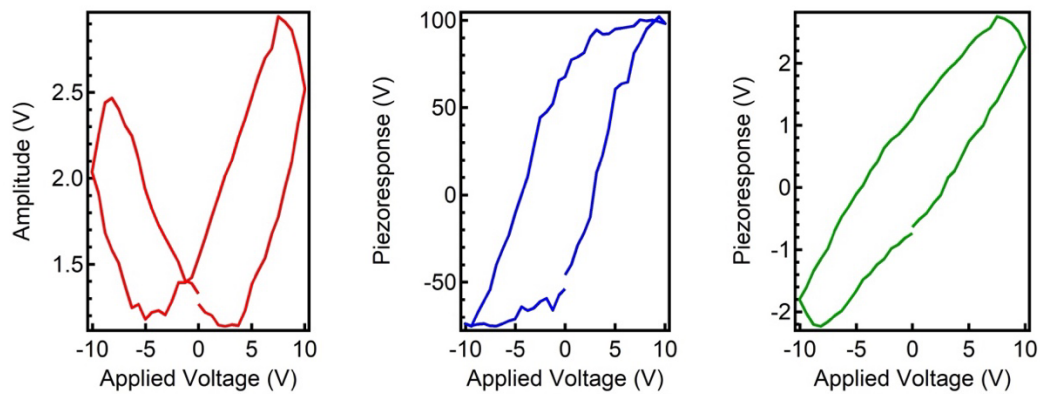

Figure A1 the PFM analysis of a standard PZT sample as a function of the applied voltage (V).

The amplitude loop shows the relationship between the applied voltage (V) and the amplitude (V) of the piezoresponse. The "butterfly" shape is observed, which is typical for ferroelectric materials like PZT. The phase loop displays clear hysteresis loop, indicating the switching of polarization states within the PZT sample. The phase changes sharply as the voltage is applied, which is a hallmark of ferroelectric behavior. The loop piezoelectric response (V) versus the applied voltage (V).

The distinct loop further confirms the ferroelectric nature of the PZT sample, demonstrating the switching behavior of the polarization states. For summary, these results verify that our PFM setup is properly configured and functioning correctly. By measuring the PZT sample, we have confirmed the setup's ability to accurately detect and measure ferroelectric properties. The clear amplitude, phase, and piezoresponse loops consistent with expected ferroelectric behavior indicate that our system is well-calibrated and reliable for studying ferroelectric materials. This validation is crucial for ensuring that subsequent measurements on other samples, such as BFO films, will be accurate and trustworthy.

A.2   Piezoresponse force microscope (PFM) under light irridation

A.2.1 Amplitude Phase after poling +10 V and -10V in different UV states
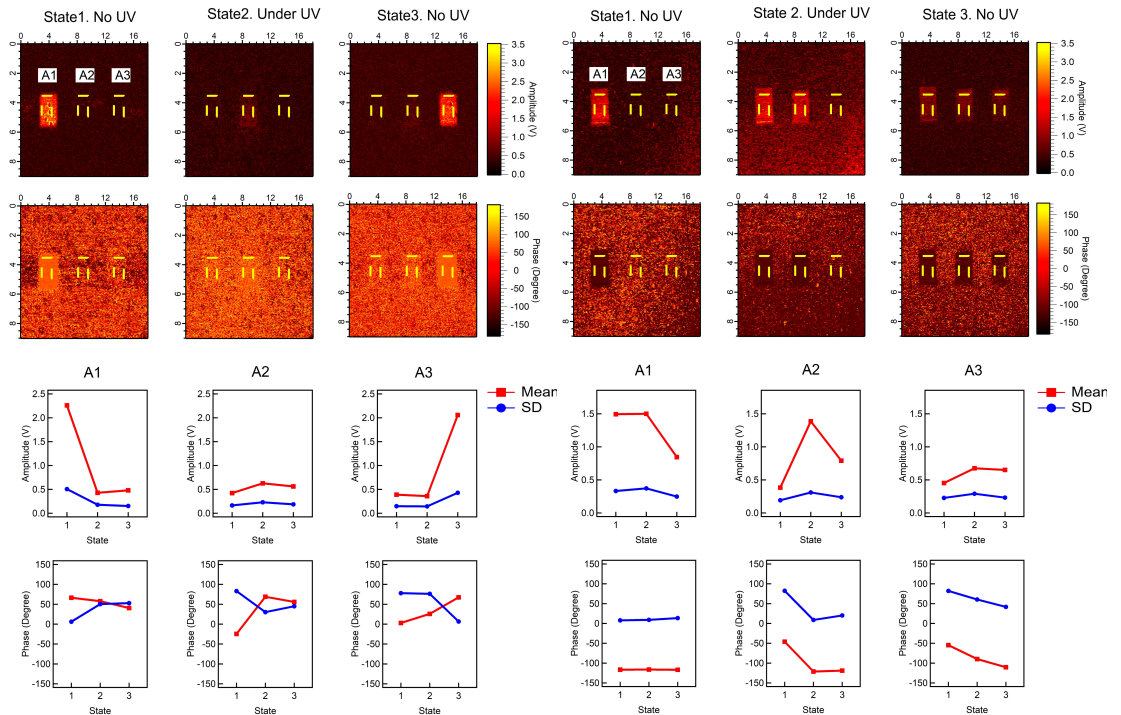

Figure A2 PFM amplitude measurements of BFO/NSTO annealed under different UV states: No UV (State 1), Under UV (State 2), and After UV (State 3). The top row displays the PFM amplitude images for each state, while the bottom row shows the mean and standard deviation (SD) of the amplitude for three areas (A1, A2, and A3) across the different states.

A.2.2 PFM Amplitude and phase measurements of BFO/NSTO annealed over time under No UV and Under UV conditions

These results display the PFM amplitude and phase images over time, with -10V and +10V poling under no UV and UV conditions, respectively. The graphs show the mean and standard deviation of amplitude and phase plotted against time at 1, 2, 4, 6, 8, and 10 minutes.
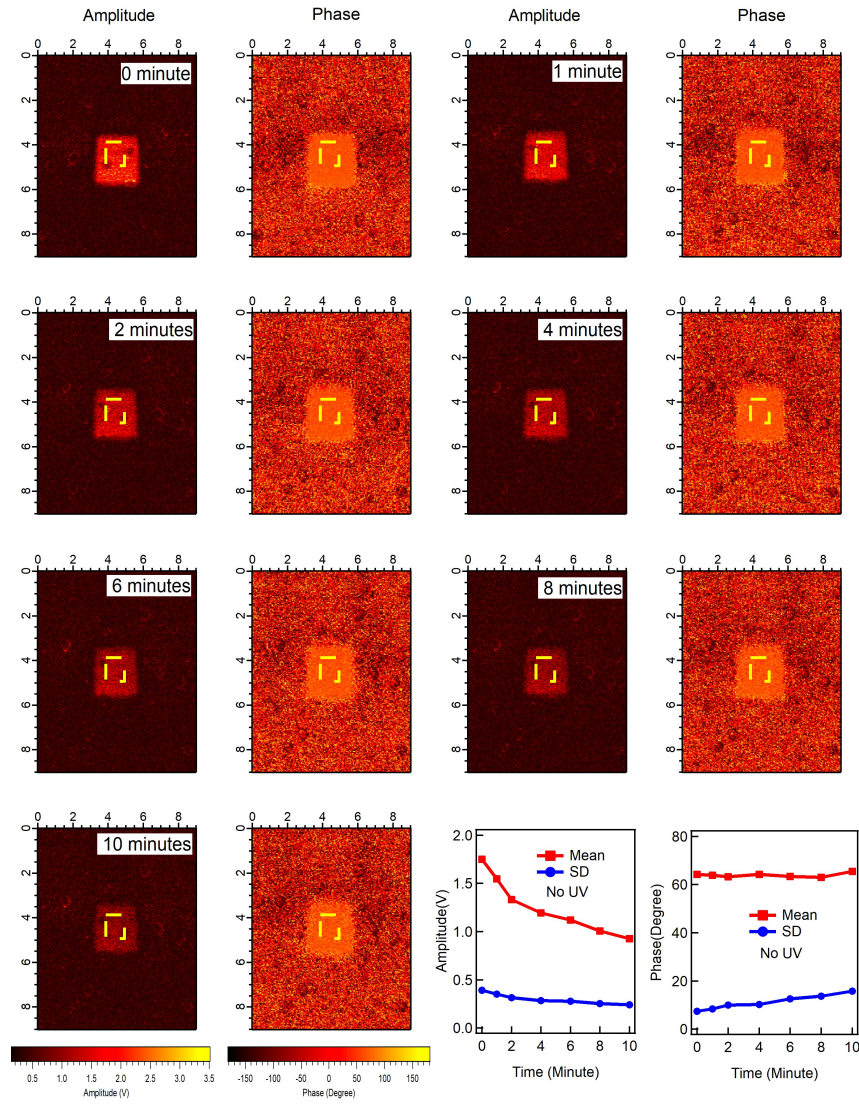

Figure A3 PFM amplitude and phase measurements of BFO/NSTO annealed over time with -10V poling under No UV.
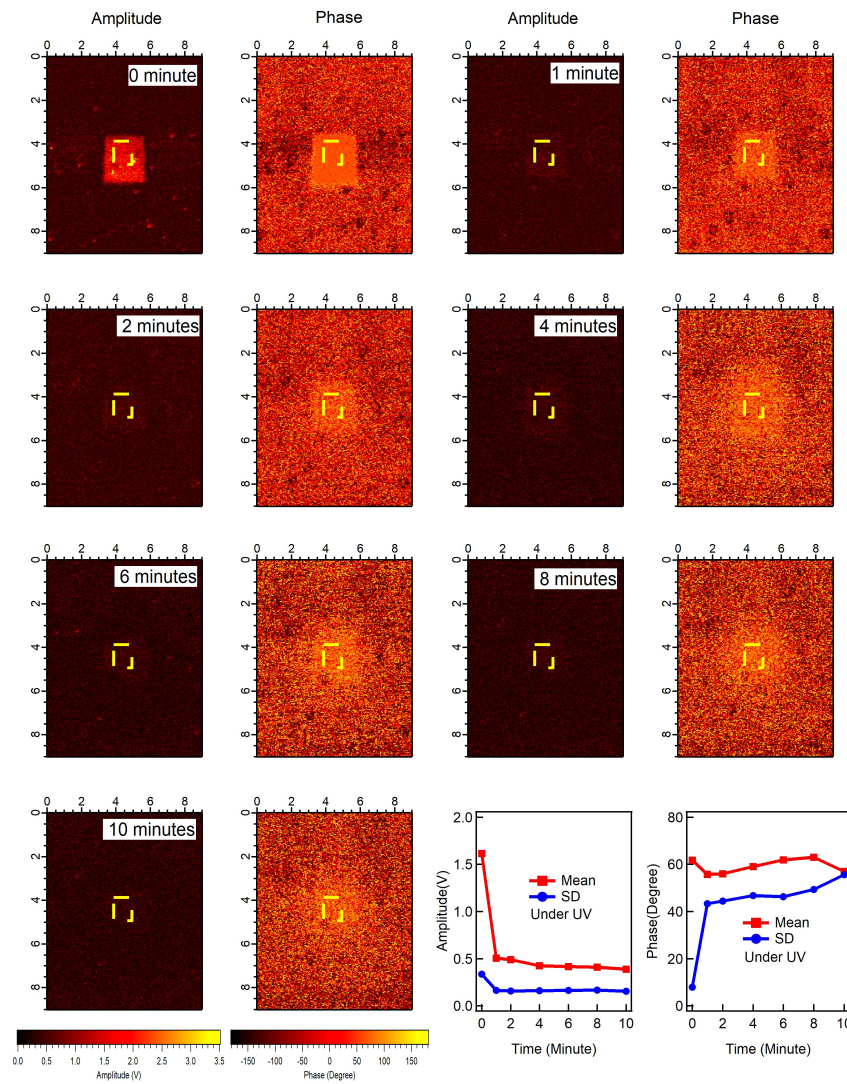
Figure A4 PFM amplitude and phase measurements of BFO/NSTO annealed over time with -10V poling under UV conditions.
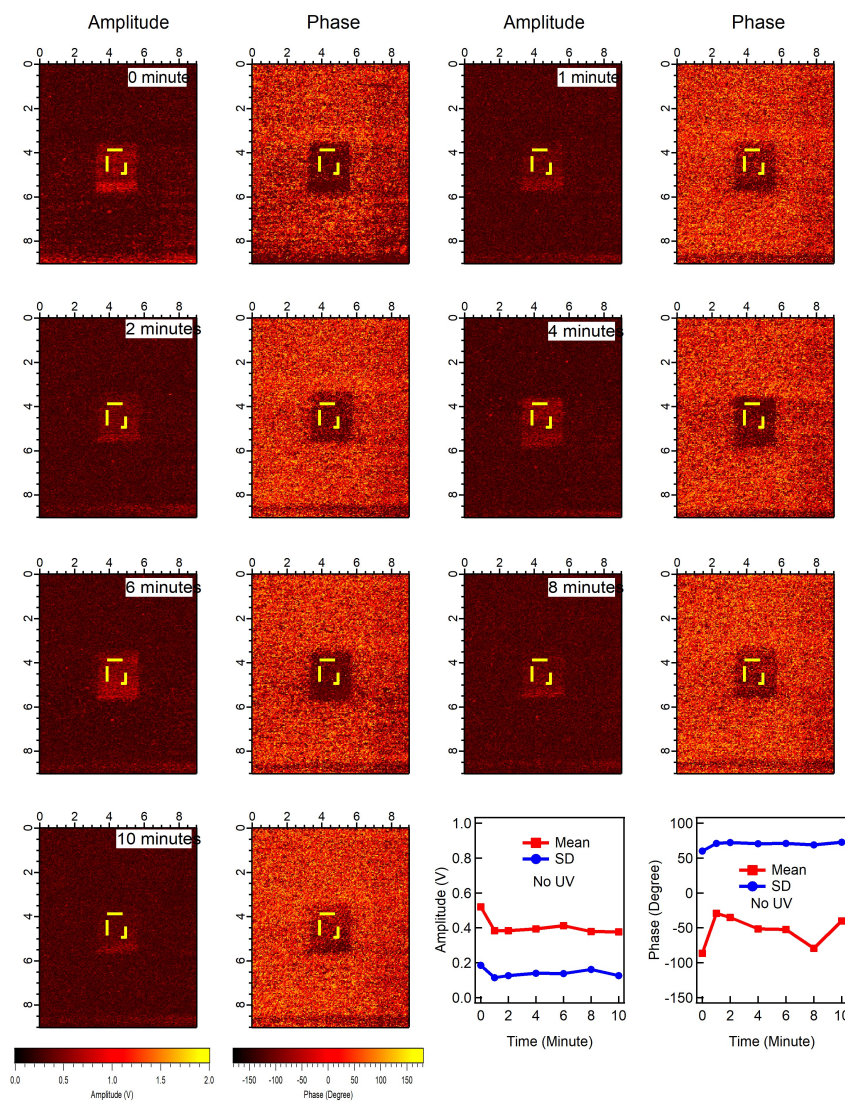
Figure A5 PFM amplitude and phase measurements of BFO film on NSTO over time with +10V poling under No UV conditions.
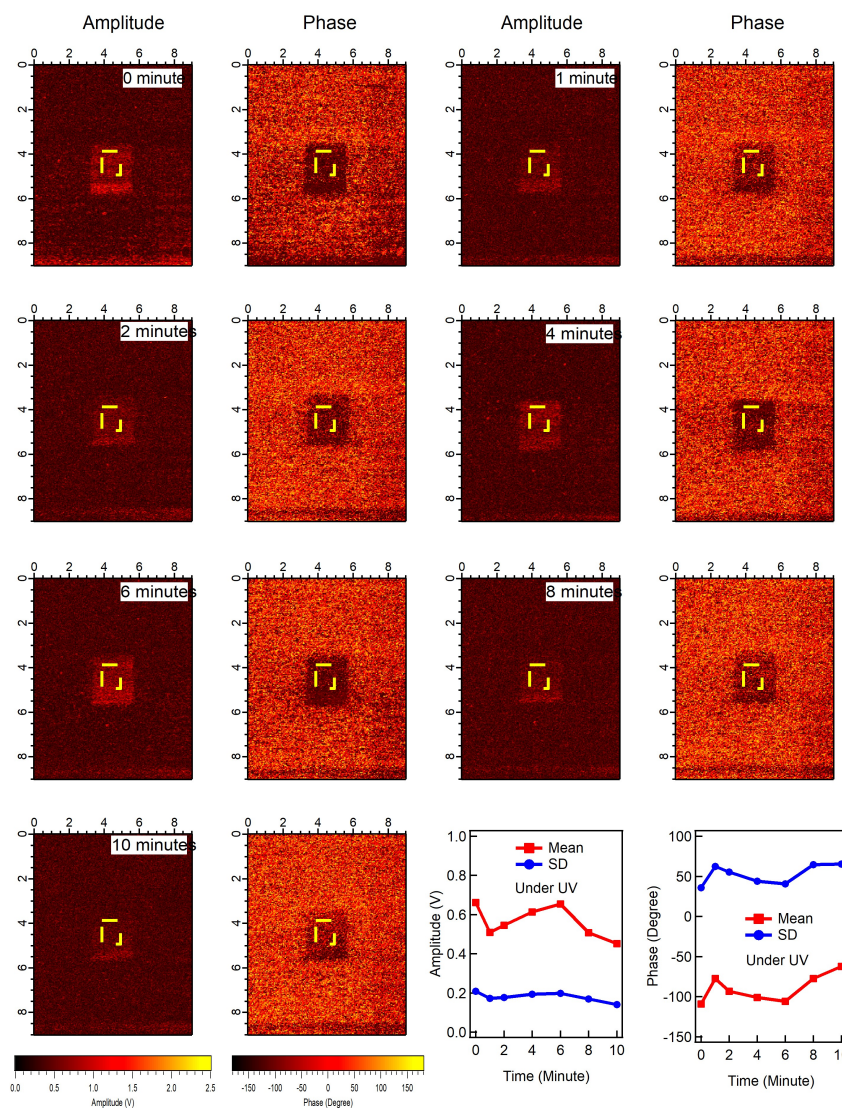
Figure A6 PFM amplitude and phase measurements of BFO film on NSTO over time with +10V poling Under UV conditions.
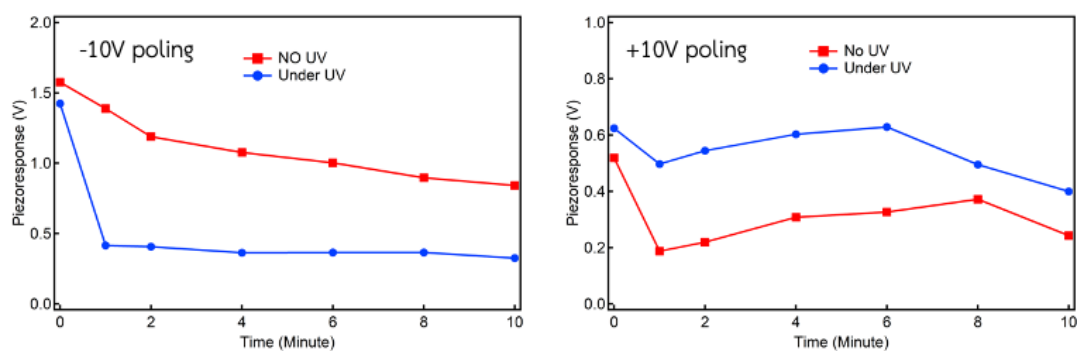

Figure A7 piezoresponse over time of BFO film on NSTO over time with -10V and +10V poling Under no and UV conditions.

The PFM measurements on BFO/NSTO samples annealed at 600°C for 30 minutes reveal significant effects of UV exposure on polarization dynamics. Under -10V poling, the piezoresponse decreases steadily without UV, indicating gradual depolarization. However, with UV exposure, the piezoresponse drops sharply within the first minute, stabilizing at a much lower value. This suggests that UV light accelerates depolarization. For +10V poling, the piezoresponse initially decreases in the first minute, increases from 2 to 8 minutes, and then decreases again at 10 minutes without UV. With UV exposure, the pattern is similar but with reduced changes in piezoresponse. This indicates that UV light enhances the stability of the polarization, causing less variation compared to the no-UV condition. In conclusion, UV exposure can be used to effectively control the polarization states in BFO/NSTO samples. It rapidly removes polarization under -10V poling and enhances stability under +10V poling. These findings highlight the potential of UV light for tuning ferroelectric properties, useful for applications in memory devices and sensors.
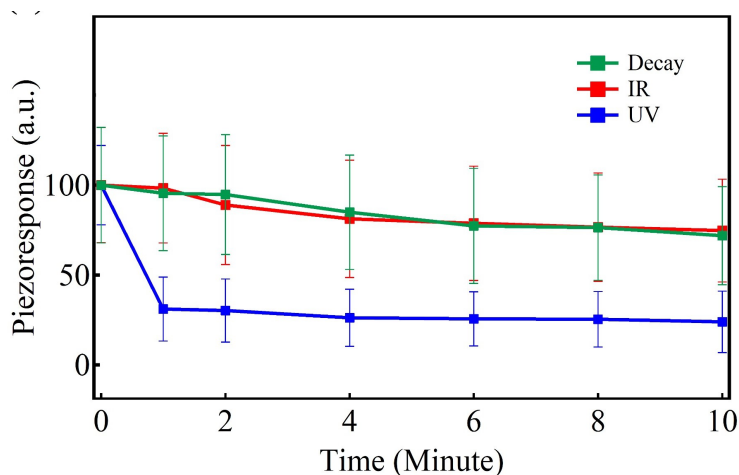
Figure A8 Plot of piezoresponse as a function of time for the annealed BFO/NSTO sample under three conditions: natural decay in darkness (green), infrared (IR) illumination (red), and UV illumination (blue).

To study the effect of UV light, piezoresponse measurements were carried out on BFO/NSTO samples under three different conditions: natural decay in the dark, IR illumination, and UV illumination. The samples were poled using a −10 V DC voltage, and the measurements were taken at 1, 2, 4, 6, 8, and 10 minutes, as

shown in Figure A8. The piezoresponse values were converted into percentages and normalized to the initial value at time zero. This helps to clearly compare how the signal changes over time in each condition. Under natural decay (green), the piezoresponse gradually decreases, which reflects typical relaxation behavior of the material. With IR light (red), the trend is similar, showing about a 25% drop after 10 minutes. This suggests that heat has only a small effect on the polarization. However, when exposed to UV light (blue), the piezoresponse drops sharply by 70% in the first minute, then continues to decrease more slowly. This fast drop suggests that UV light speeds up the breakdown of the ferroelectric properties in a way that heat alone cannot explain.
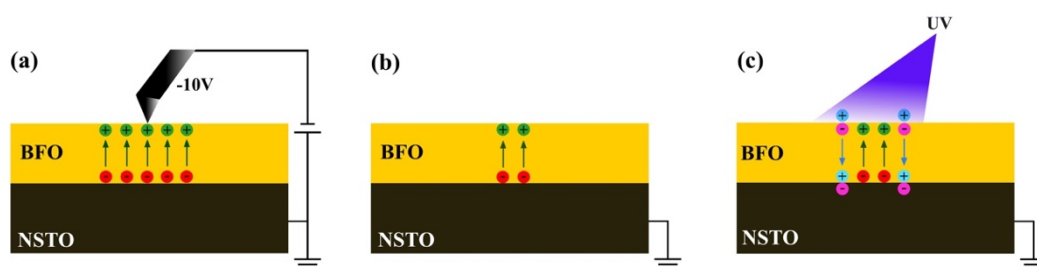
Figure A9 Schematic diagram showing the DC poling process and the effect of UV light on oxygen vacancy formation at the BFO/NSTO interface: (a) −10 V poling with indicated polarization direction, (b) the state before UV exposure, and (c) the state after UV exposure.

The effect of DC poling and UV illumination on charge distribution, polarization behavior, and the formation of a two-dimensional electron gas (2DEG) at the BFO/NSTO interface is illustrated in Figure A9. The green and red symbols represent the polarization charges generated by DC poling, while the blue and pink symbols show the charges induced by UV light. When a −10 V DC voltage is applied, the polarization in the BFO layer points upward. This causes positive bound charges to accumulate on the top surface of the BFO and negative bound charges to appear at the BFO/NSTO interface, as shown in Figure A9(a). This arrangement reflects a stable

ferroelectric state under the external field. Since NSTO is conductive and not ferroelectric, it supports the redistribution of charges rather than contributing to polarization itself. Over time, without UV light, the polarization gradually weakens due to processes such as charge recombination, depolarization, and intrinsic screening effects, as illustrated in Figure A9(b). However, when UV light is applied, oxygen vacancies form in the BFO and at the interface. These vacancies act as donor-like states that release free electrons. The electrons accumulate at the BFO/NSTO interface, leading to the formation of a 2DEG and enhancing local conductivity. These free carriers also screen the polarization field, resulting in a rapid drop in polarization amplitude. This sharp decline highlights the strong interaction between UV-induced charge carriers and the ferroelectric stability of the material, as shown in Figure A9(c). Interestingly, once the UV light is turned off, a partial recovery of the polarization amplitude is observed, suggesting a short-term and reversible process in addition to possible long-term structural changes. During UV exposure, photoexcited electron–hole pairs are also generated within the BFO layer. These carriers are redistributed by the internal depolarization field, creating an internal electric field that opposes the existing remanent polarization caused by DC poling. As a result, the net polarization amplitude temporarily decreases during UV exposure.

A. 3   Experimental set up measurement

A.3.1   PFM Commercial Setup
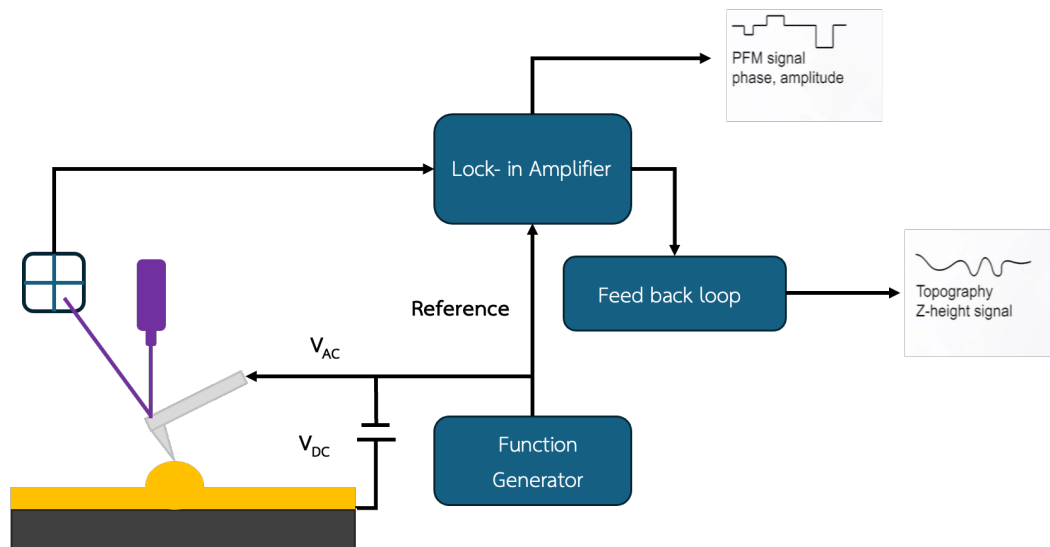
Figure A10 Commercial setup for PFM measurements.

In the PFM commercial setup, the process starts with the function generator, which creates an AC voltage signal. This voltage is applied to the sample through the conductive tip of an AFM (Atomic Force Microscope). The sample, if piezoelectric, responds to this voltage by mechanically deforming. The tip, in contact with the sample surface, detects these mechanical deformations. The cantilever's deflection, caused by the sample's response, is monitored to gather data on the sample's piezoelectric properties. A lock-in amplifier was used to process the signals from the cantilever. It extracts specific amplitude and phase information from the piezoresponse signal while filtering out noise, which ensures that the measurements are accurate and reliable. This processed signal provides detailed insights into the sample's piezoelectric behavior. The feedback loop is another essential component. It maintains a constant force between the AFM tip and the sample surface, ensuring that the tip remains in consistent contact with the sample throughout the scanning process. This consistency is vital for accurate data collection. As the AFM tip scans across the sample, it records mechanical deformations. These deformations are then

processed to produce two main types of data: the PFM signal (which includes phase and amplitude information) and the topography (Z-height signal), which details the surface structure of the sample. This comprehensive data allows researchers to generate detailed images that showcase both the piezoelectric properties and the surface features of the sample, providing a thorough understanding of its material characteristics.

A.3.2   PFM Hysteresis loop set up
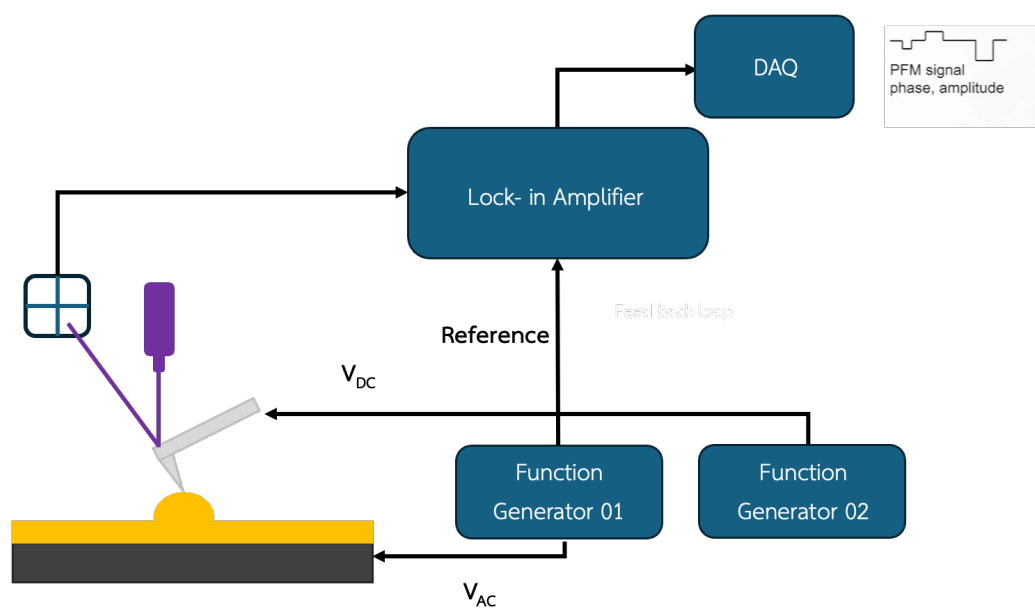
Figure A11 PFM Hysteresis loop setup.

The PFM hysteresis loop measurement setup, as depicted in the figure, involves several key components: two function generators, a lock-in amplifier, a DAQ (Data Acquisition) system, and a feedback loop. This configuration is designed to analyze the ferroelectric properties of a sample. The two function generators produce AC voltages and triangle DC voltage that are applied to the sample and the conductive AFM tip, respectively. Similar to commercial setup, the lock-in amplifier processes the deformations detected by the AFM tip to measure the amplitude and phase of the piezoresponse signal accurately. The DAQ system records these lock-in processed PFM data that provide detailed insights into the sample's ferroelectric properties, including PFM amplitude, phase, and piezoresponse as a function of applied DC voltage. As

result of that, hysteresis loops can be described. Additionally, the study investigates the coercive field and remanent polarization.
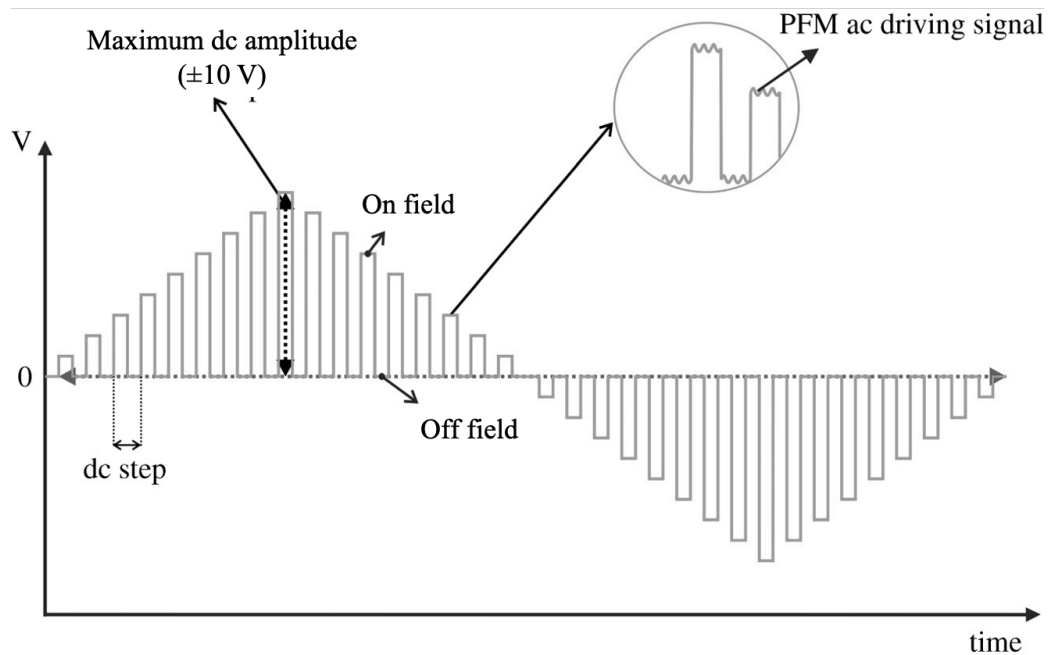
Figure A12 Piezoresponse over time of BFO film on NSTO over time with -10V and +10V poling Under no and UV conditions.

The waveform has a distinctive triangular shape, where the voltage ramps up linearly to a maximum value and then ramps down linearly to a minimum value. This cyclical pattern ensures that the sample experiences a full range of electric field strengths. The waveform reaches a maximum amplitude of ±10 V. This wide range of applied voltages helps in polarizing the sample thoroughly, making it possible to observe the complete hysteresis behavior. The voltage increases in discrete steps rather than continuously. These steps allow for precise control and measurement at each voltage level. When the voltage is actively increasing or decreasing, the sample is in the on-field period. During this time, the electric field is actively changing the polarization state of the sample. After each step of the voltage increase, the field is momentarily turned off. These off-field periods are critical as they provide snapshots of the sample's response without the influence of an external field.

The amplitude and phase of the piezoresponse signal at each voltage step. The lock-in amplifier processes these signals to ensure accuracy. The most important data points are collected during the off-field periods. These measurements capture the sample's inherent piezoelectric response, unaffected by the applied field. The amplitude and phase data obtained during the off-field periods are used to construct a hysteresis loop. This loop illustrates the relationship between the piezoresponse and the applied voltage. The key features of the hysteresis loop include coercive field and remanent polarization. Coercive field is the electric field at which the polarization reverses. Remanent Polarization is the residual polarization remaining after the external field is removed.

A.3.3   Data acquaintance and analysis algorithms

Both data acquaintance and analysis were performed by python code with numpy, pandas, matplotlib and nidaqmx libraries. Some inhouse (SSPFM) and commercial (Keysight_33600A, Agilent) codes were used to build the desired waveform and to control the waveform generator. The result that came from lock-in amplifier will be described as a "raw data" here. Additionally, the main code was used to obtain the raw data and process it described in Figure A10. In each point of measurement, the raw data will be read through data acquaintance channel including applied voltage, PFM amplitude and PFM phase. Reference waveform will be utilized to map out the on-field and off-field region on applied voltage. For each applied voltage, raw data will be processed by averaging values on the off-field region. The main code notebook is available here:

https://drive.google.com/drive/folders/1PJg84mA_cWdOn07xlX2zU1smxuM1yJvO?usp=sharing.
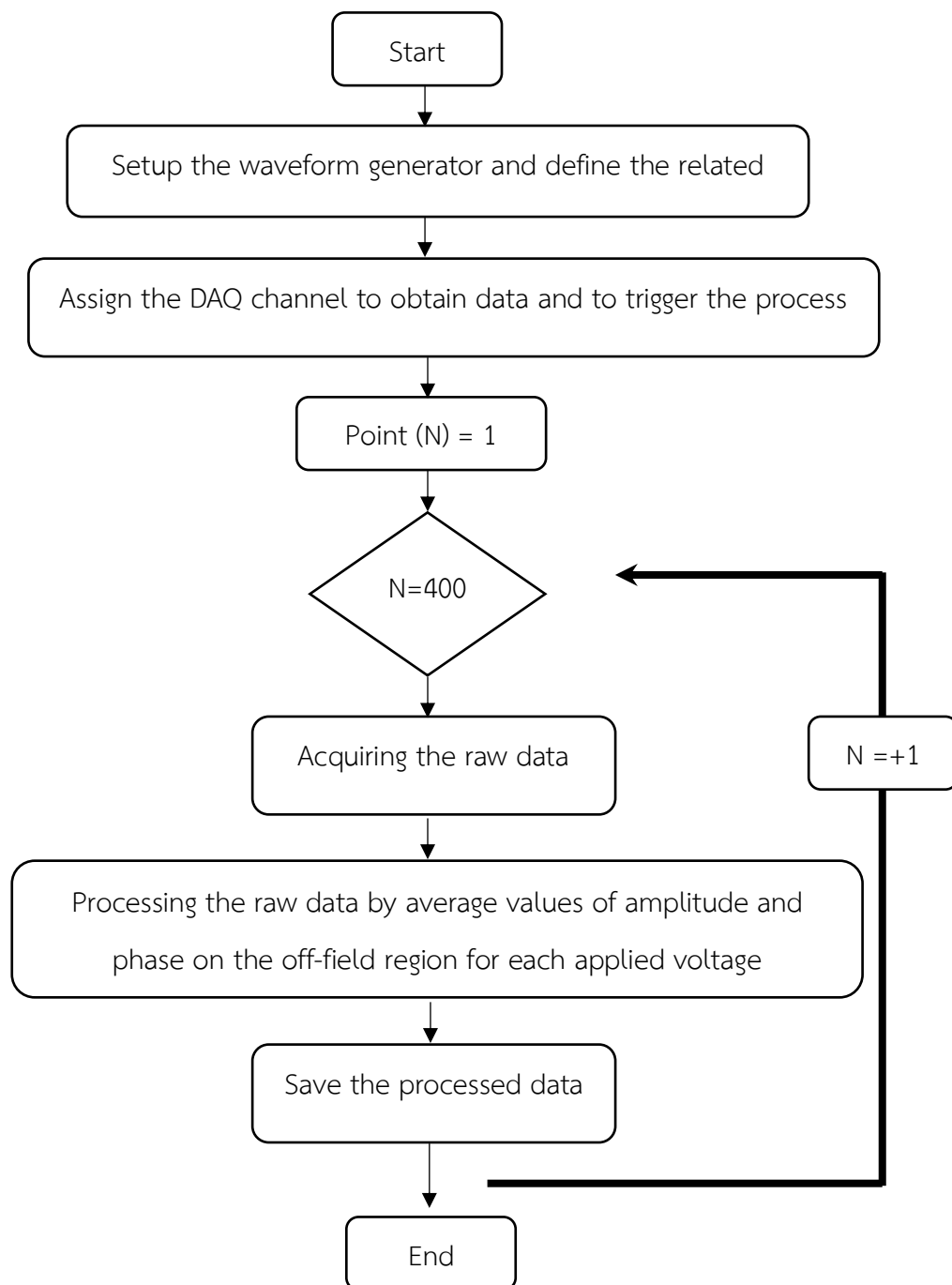
```
                    ┌───────────────┐
                    │     Start     │
                    └───────┬───────┘
                            │
                            ▼
    ┌───────────────────────────────────────────────────┐
    │ Setup the waveform generator and define the related│
    └───────────────────────┬───────────────────────────┘
                            │
                            ▼
    ┌───────────────────────────────────────────────────┐
    │ Assign the DAQ channel to obtain data and to       │
    │ trigger the process                                │
    └───────────────────────┬───────────────────────────┘
                            │
                            ▼
                    ┌───────────────┐
                    │  Point (N) = 1│
                    └───────┬───────┘
                            │
                            ▼
                    ◇───────────────◇
                    │    N=400      │◄──────────────┐
                    ◇───────────────◇               │
                            │                       │
                            ▼                  ┌──────────┐
    ┌───────────────────────────────────────┐ │  N =+1   │
    │         Acquiring the raw data         │ └──────────┘
    └───────────────────────┬───────────────┘      ▲
                            │                       │
                            ▼                       │
    ┌───────────────────────────────────────────────────┐
    │ Processing the raw data by average values of       │
    │ amplitude and phase on the off-field region for    │
    │ each applied voltage                               │
    └───────────────────────┬───────────────────────────┘
                            │
                            ▼
                    ┌───────────────┐
                    │Save the processed data│──────────┘
                    └───────┬───────┘
                            │
                            ▼
                    ┌───────────────┐
                    │      End      │
                    └───────────────┘
```

Figure A13 Data acquaintance and analysis algorithms.

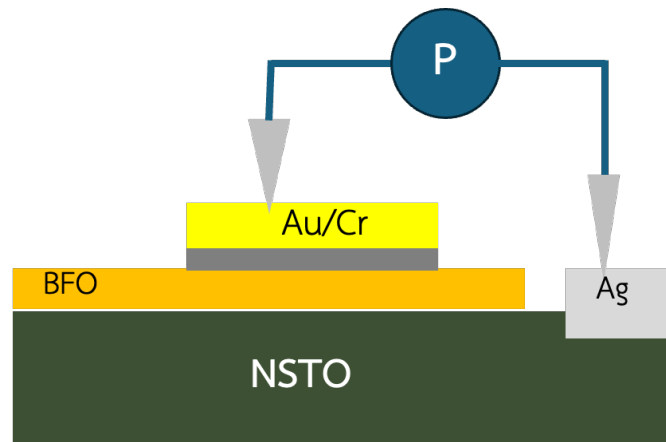### A.3.4   P-E loop sample configuration

Figure A14 Sample configuration for P-E loop measurement. The setup includes an NSTO substrate, a BFO thin film, Au/Cr layer, and Ag bottom electrode.

The sample configuration for P-E loop measurement is designed to study the ferroelectric properties of BFO thin films. The base layer is an NSTO substrate, which is conductive. On top of this substrate, a thin film of BFO is deposited. BFO is the material whose ferroelectric properties we want to measure. The top electrode is a layer of Au with a layer of Cr underneath. Gold is used because it is a good conductor and does not react easily with other chemicals. Cr helps the gold stick better to the BFO film. The bottom electrode is made of Ag paste, which is in contact with the NSTO substrate. During the PE loop measurement, an electric field is applied across the BFO layer using the Au top electrode and the Ag bottom electrode. The changes in polarization in the BFO layer are measured by the piezoresponse measurement system.

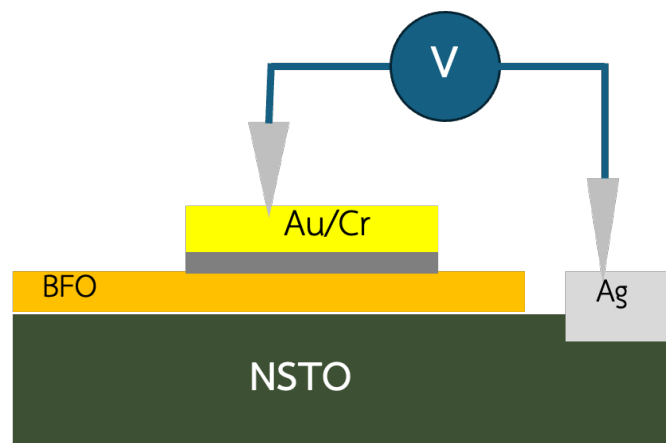### A.3.5 Voltage measurement sample configuration

Figure A15 Voltage measurement sample configuration.

The sample configuration is similar to the P-E loop measurement setup. we measure voltage using a multimeter. Voltage measurements are taken under no UV and under UV conditions to observe the effects of UV light on the BFO thin film.

APPENDIX B

PUBLICATIONS AND PRESENTATIONS

B.1   List of publications

B.1.1   Co-first author

Mooltang, A., Sriboriboon, P., Thooppanom, N., Jindata W., Tepakidareekul, M., Srisom K., Sangtawesin, S., Janphuang, P., and Meevasana, W. (2025), Voltage-tuned polarization control via UV light in $BiFeO_3$ thin film on $Nb–SrTiO_3$. *APL Mater*, 13, 071114.

Chaiyachad, S., Kaeokhamchan, Y., Mooltang, A., Chuewangkam, N., Pinitsoontorn, S., Janphuang,P., Meevasana, W. (2023), Enhanced and Tuneable Ferromagnetism in CVD Synthesized Metasurface Carbon Films. *Research Square*.

B.2   List of oral presentation

Mooltang, A., Sriboriboon, P., Thooppanom, N., Jindata W., Tepakidareekul, M., Srisom K., Sangtawesin, S., Janphuang, P., Meevasana, W. (2025), The 5th Materials Research Society of Thailand (MRS-Thailand 2025). Bangkok, Thailand

Mooltang, A., KriSrisom, K., Rasritat, A., Laohana, P., Chaiyachad,S., and Meevasana, W. (2024), Science Postgrad Annual Research Conference (2nd SPARC). Nakhon Rachsima, Thailand

Mooltang, A., KriSrisom, K., Rasritat, A., Laohana, P., Chaiyachad,S., and Meevasana, W. (2024), Science Postgrad Annual Research Conference (1st SPARC). Nakhon Rachsima, Thailand.

B.3   List of poster presentation

Mooltang, A., Meevasana, W. (2021), Nanoscale Patterning of Metal Oxide Thin Films Prepared by Electron Beam Lithography for Quantum Devices. International Union of Materials Research Societies- International Conference in Asia (IUMRS-ICA). Chiang Mai, Thailand.

Mooltang, A., Siriroj, S., and Meevasana, W. (2019), Nanoscale Patterning of Metal Oxide Thin Films Prepared by Electron Beam Lithography for Quantum Devices. The 2nd Materials Research Society of Thailand International Conference. Chonburi, Thailand.

Mooltang, A., Siriroj, S., Thongbai, P., and Meevasana, W. (2017), Study of $CaCu_3 Ti_4 O_{12}$ (CCTO) in liquid system under irradiate by laser. The First Materials Research Society of Thailand International Conference. Chiang Mai, Thailand.